

Polyacrylonitrile Single-Walled Carbon Nanotube Composite Fibers**

By Thaliyil V. Sreekumar, Tao Liu, Byung G. Min, Huina Guo, Satish Kumar,* Robert H. Hauge, and Richard E. Smalley

Single-walled carbon nanotubes (SWNTs) have a high tensile strength and modulus.^[1] SWNT-reinforced pitch-based carbon fibers have significantly improved mechanical properties as compared to the unmodified pitch-based fibers.^[2] Increased thermal stability, glass transition temperature, and storage modulus with the incorporation of carbon nanotubes in various polymer matrices have been reported.^[3] Poly(*p*-phenylene benzobisoxazole) (PBO)/SWNT composite fibers containing 10 wt.-% SWNTs of greater than 99 % purity exhibited 50 % higher tensile strength as compared to the control PBO fiber.^[4] Excellent evidence of load transfer using Raman spectroscopy has been observed in poly(vinyl alcohol)/SWNT composite system.^[5] Polyacrylonitrile (PAN) copolymers are commercially important,^[6] and are used as carbon fiber precursors,^[7] as well as for developing porous and activated carbon for a variety of applications, including catalysis, electrochemistry, separation processes, energy storage devices, etc.^[8] Films have been made from PAN/MWNT (MWNT = multi-walled carbon nanotube) homogeneous dispersions.^[9] SWNTs can be dispersed in solvents such as dimethylformamide (DMF) and dimethylacetamide (DMAc).^[10] Carbonized and activated PAN/SWNT films are very promising for supercapacitor electrode application.^[11] In this work solution spun PAN/SWNT fibers containing 10 wt.-% nanotubes exhibit a 100 % increase in tensile modulus at room temperature and an order of magnitude increase at 150 °C (Table 1 and Fig. 1), significant reduction in thermal shrinkage as well as polymer solubility, and a 40 °C increase in the glass transition temperature (Fig. 1) as compared to the control PAN fiber. These observations provide evidence of interaction between PAN and SWNTs. SWNTs exhibit higher orientation than PAN, as determined by Raman and X-ray

Table 1. Properties of PAN and PAN/SWNT composite fibers.

SWNT [wt.-%]	Fiber cross-sectional area [cm ²]	Tensile modulus [GPa]	Tensile strength [GPa]	Elongation at break [%]	T _g [°C]
0	4.4 × 10 ⁻⁵	7.9 ± 0.4	0.23 ± 0.03	11.6 ± 1.4	103
5	3.9 × 10 ⁻⁵	14.2 ± 0.6	0.36 ± 0.02	11.9 ± 1.3	114
10	4.9 × 10 ⁻⁵	16.2 ± 0.8	0.33 ± 0.02	9.7 ± 1.6	143

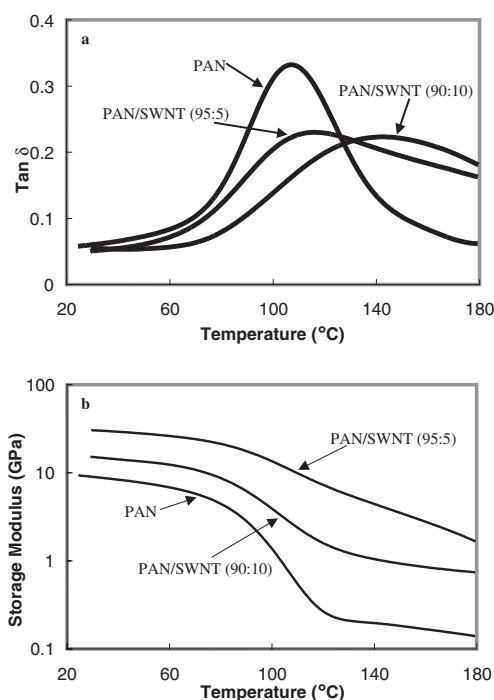


Figure 1. a) $\tan \delta$ and b) storage modulus as a function of temperature for PAN and PAN/SWNT composite fibers.

diffraction, respectively. SWNT anisotropy in the composite fiber has also been studied using infrared spectroscopy. The observed modulus of the composite fiber is consistent with theoretical predictions.

The glass transition temperature ($\tan \delta$ peak position) increased from ~103 °C for the control PAN fiber to above 143 °C for the PAN/SWNT (90:10) fiber, the magnitude of the $\tan \delta$ peak decreased significantly, and the $\tan \delta$ peak broadened towards higher temperatures (Fig. 1a). The motion of PAN molecules closer to the SWNT would be more constrained than those farther away from it. The broadening of the $\tan \delta$ peak to higher temperatures is attributed to this variation in interaction between PAN and SWNTs. The room-temperature modulus of PAN/SWNT (90:10) fiber is nearly twice that of the control PAN fiber, while the modulus retention at 150 °C is improved by more than an order of magnitude (Fig. 1b).

At 200 °C, shrinkage in the PAN/SWNT (90:10) composite fiber is nearly half of the shrinkage in the control PAN fiber (Figure 2). The shrinkage in the PAN fiber up to about 200 °C is mostly entropic. PAN molecules interacting with the SWNTs are not as free to shrink as in the absence of nano-

[*] Prof. S. Kumar, Dr. T. V. Sreekumar, Dr. T. Liu, Prof. B. G. Min,^[+] H. Guo

School of Polymer, Textile and Fiber Engineering
Georgia Institute of Technology, Atlanta, GA 30332 (USA)
E-mail: satish.kumar@ptfe.gatech.edu

Dr. R. H. Hauge, Prof. R. E. Smalley
Center for Nanoscale Science and Technology
Rice University, Houston, TX 77005 (USA)

[+] Permanent address: School of Advanced Materials and System Engineering, Kumoh Institute of Technology, Kumi 730-701, Korea.

[**] This work was supported by the Office of Naval Research (N00014-01-1-0657), Carbon Nanotechnologies, Inc., and the Air Force Office of Scientific Research (F49620-00-1-0147 and F49620-03-1-0124). Support at Rice University for developing the HiPco process from NASA, the Office of Naval Research, the Texas Advanced Technology Program, and the Robert A. Welch Foundation is also acknowledged.

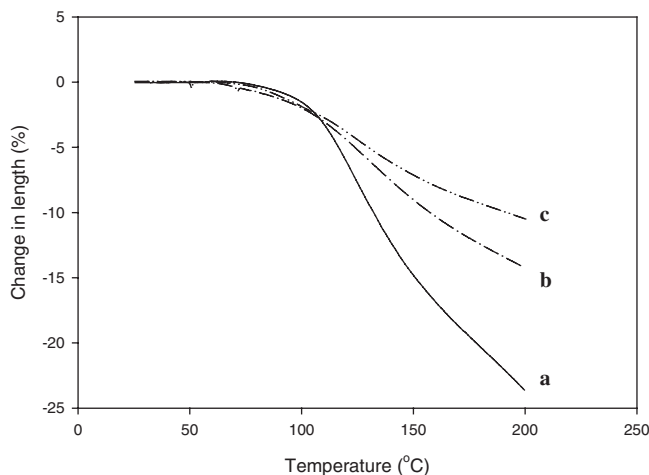


Figure 2. Thermal shrinkage in a) PAN, b) PAN/SWNT (95:5), and c) PAN/SWNT (90:10) composite fibers as a function of temperature.

tubes. The shrinkage behavior of the composite fibers is consistent with the dynamic mechanical properties data in the sense that both results suggest good interaction between PAN and SWNT. The reduced shrinkage in PAN/SWNT fibers may also be important for carbon fiber processing. Stabilization of the PAN precursor fiber in oxidative environments, typically in the 200 to 300 °C temperature range, is an important step for the processing of carbon fibers. To obtain high-modulus carbon fibers, stabilization is carried out under tension to minimize shrinkage. PAN/SWNT fibers, which exhibit inherently reduced shrinkage, may either reduce the tension requirement or result in fibers with higher orientation and ultimately higher modulus. Reduced thermal shrinkage has also been observed in poly(methyl methacrylate)/carbon nanofiber composite fibers.^[12]

Fiber tensile fracture results in significant fibrillation in the control PAN fiber, while the composite fiber exhibited no fibrillation but showed longitudinal splitting. A PAN fiber readily dissolves in DMF and DMAc, while a PAN/SWNT composite fiber did not dissolve even after several days at room temperature. Rather, it disintegrated into millimeter- and sub-millimeter-sized particles. The filtered (Fisherbrand Filter Paper, P5) solvent was colorless, suggesting that no nanotubes dissolved. Fourier transform infrared (FTIR) analysis confirmed the presence of PAN in the solvent. Based on the residual weight analysis, it was estimated that only about 50 % of the PAN in a PAN/SWNT (95:5) composite fiber dissolved. PAN–SWNT interaction prevents its complete dissolution. However, the chemical or morphological nature of this interaction has not yet been investigated.

SWNT Herman's orientation factors (f), which are given by

$$f = \frac{3\langle \cos^2 \theta \rangle - 1}{2} \quad (1)$$

where θ is the angle between the SWNT and the fiber axis, determined from Raman spectroscopy with 1, 5, and 10 wt.-% SWNTs, were 0.90, 0.94, and 0.92, respectively. The SWNT

anisotropy was also observed using infrared spectroscopy (Fig. 3). PAN fiber spectra for the two polarization directions are comparable, while the composite fiber spectra with 1 wt.-% nanotubes show significant difference in the two

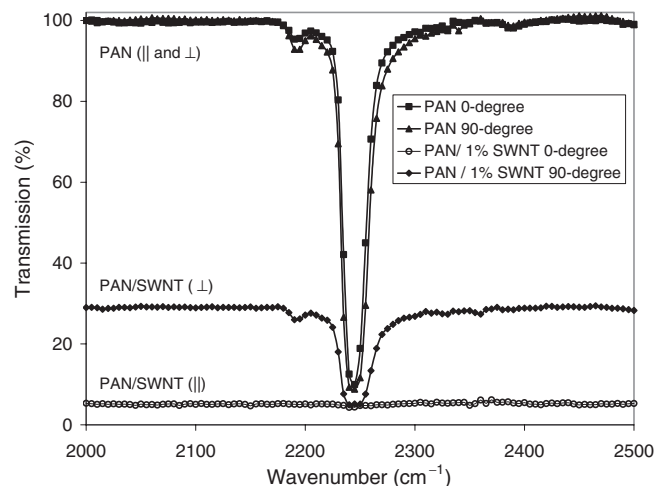


Figure 3. Polarized infrared spectra of PAN and PAN/SWNT (99:1) composite fibers.

polarization directions. For the 5 wt.-% nanotube fiber, absorption even for the perpendicularly polarized beam was very high and no transmitted beam could be observed. The SWNTs show much higher absorption when the electric field of the incident wave is parallel to the tube axis. This absorption behavior of SWNTs can be used to develop polymer/SWNTs composites with tailored absorption characteristics for the electromagnetic waves, particularly at low SWNT concentration (<1 wt.-%).

Wide-angle X-ray diffraction (WAXD) showed no diffraction peaks corresponding to SWNTs. The crystallite size from (1,0) PAN equatorial peak, determined using the Scherrer equation,^[13] was 5.6 nm for PAN as well as for the 5 and 10 wt.-% composite fibers. From the azimuthal scans (at $2\theta = 16.8^\circ$), the Herman's orientation factors for the (1,0) diffraction peak were determined to be -0.29 , -0.34 , and -0.33 for the PAN, and 5 and 10 wt.-% composite fibers, respectively. Based on this,^[14] the PAN orientation factor along the chain axis can be estimated to be 0.58, 0.68, and 0.66 for the PAN, 5 and 10 % PAN/SWNT fibers, respectively. A comparison of orientation factors show that in the composite fiber, SWNTs have higher orientation than PAN. This is attributed to higher rigidity and lower relaxation times for SWNTs as compared to PAN.

Now we consider the reinforcement efficiency of SWNTs. Mechanical properties of a two-phase composite, in which both the matrix and the reinforcement have different orientation,^[15] requires a full set of elastic constants for the anisotropic matrix, which are currently not available for PAN. Therefore the composite fiber modulus (E_c) was estimated using the equation,

$$E_c = V_{NT}E_{NT} + V_{PAN}E_{PAN} \quad (2)$$

where E_{NT} and E_{PAN} are the nanotube and PAN moduli along the fiber axis, and V_{NT} and V_{PAN} are their volume fractions, respectively. Based on the SWNT orientation factors for 5 and 10 wt.-% composite fibers, and the orientation dependence of the SWNT modulus, E_{NT} values obtained from the literature^[16] for two different rope diameters are listed in Table 2, along with values of E_{PAN} , V_{NT} , and V_{PAN} . Table 2 shows that the experimental values are well within the predicted modulus

Table 2. Physical and mechanical properties of SWNT/PAN composite fibers.

	PAN	PAN/SWNT (95:5 wt.-%)	PAN/SWNT (90:10 wt.-%)
V_{NT} [a]	0	4.6	9.2
f_{PAN} (X-ray)	0.58	0.68	0.66
f_{NT} (Raman)	-	0.94	0.92
E_{PAN} [GPa] [b]	7.9	9.4	9.1
E_{NT} [GPa] (SWNT rope diameter >20 nm) [c]	-	28.2	22.2
E_{NT} [GPa] (SWNT rope diameter ~4.5 nm) [c]	-	149.1	122.6
E_c [GPa] (SWNT rope diameter \geq 20 nm)	-	10.3	10.3
E_c [GPa] (SWNT rope diameter ~ 4.5 nm)	-	15.8	19.5
E_{exp} [GPa]	7.9	14.2	16.2

[a] V_{NT} calculated assuming PAN and SWNT densities of 1.18 g cm^{-3} and 1.30 g cm^{-3} , respectively. [b] E_{PAN} for the composite fibers was calculated from the control PAN fiber modulus to account for the difference in orientation. [c] Obtained from the literature [16] for the given f_{NT} and rope diameter.

range for the two rope diameters. The rope diameter for the SWNT powder used in this study was measured to be $37 \pm 8 \text{ nm}$ from scanning electron microscopy.^[11] However, the measured modulus is closer to the predictions based on smaller diameter ropes. This suggests that some SWNT rope exfoliation has occurred during mixing, fiber processing, and fiber drawing. Based on high-resolution transmission electron microscopy study, the average single-walled nanotube bundle diameter in a PAN/SWNT (95:5) fiber was measured to be 11 nm, confirming partial exfoliation.^[17] Further improvement in nanotube exfoliation and orientation is expected to result in further modulus increase.^[16]

In summary, SWNTs have been well dispersed in PAN solution in DMF as well as in DMAc. PAN/SWNT composite fibers exhibiting good interaction between PAN and SWNTs have been solution spun. The evidence of interaction has been obtained from increased modulus and glass transition temperature, as well as from decreased shrinkage and solubility.

Experimental

Purified high-pressure carbon monoxide (HiPco) SWNTs [18] exhibiting 7 wt.-% residue at 800 °C in air produced at Rice University, and DMF, DMAc, and polyacrylonitrile-co-methyl acrylate (P(AN/MA)) copolymers obtained from Sigma-Aldrich were used as received. The P(AN/MA) copolymer ratio is 90:10 and the polymer

molecular weight is $\sim 100\,000 \text{ g mol}^{-1}$. SWNTs, vacuum dried at 110 °C for 5 h, were mixed with excess solvent (DMF or DMAc) and sonicated at room temperature for 2 h using a bath sonicator (Cole-Parmer 8891R-DTH). During the sonication, the SWNT/solvent mixture was stirred periodically using a bio-homogenizer (Biospec Products Inc. M133/1281-0). The solution/dispersion was then transferred to a round bottom flask, and the excess solvent was boiled off to obtain the desired final SWNT/solvent volume, to which P(AN/MA) copolymer was added while stirring at $\sim 5 \text{ }^\circ\text{C}$. To obtain a 99:1 PAN/SWNT weight ratio, 0.15 g of purified HiPco SWNTs were mixed with 250 mL DMAc. Excess solvent was boiled off at 166 °C, to obtain a final SWNT/DMAc volume of about 107 mL, which weighs nearly 100 g. This SWNT/DMAc dispersion did not settle for several days; however, optical microscopy showed that this mixture was not homogeneous. To this dispersion, 14.85 g P(AN/MA) copolymer was added while stirring at $\sim 5 \text{ }^\circ\text{C}$. As compared to the SWNT/DMAc dispersion, this P(AN/MA)/SWNT/DMAc dispersion was optically homogeneous; however, a few hard SWNT particles still remained that could not be dispersed. Solutions containing P(AN/MA)/SWNT in the ratio 95:5 and 90:10 were also prepared using the same approach. P(AN/MA) copolymer has been referred to as PAN.

The fibers were dry-jet wet spun, on a small-scale spinning machine manufactured by Bradford University Research Ltd, using a single hole spinneret of 500 μm diameter. A 635 mesh (20 μm) stainless steel filter pack (from TWP Inc.) was used in the spinning process. The dope temperature was maintained at 80 °C, and the air gap (distance between the spinneret orifice and the liquid surface in the first coagulation bath) was about 5 cm. The volumetric throughput rate was 0.27 mL min⁻¹ per hole to obtain a linear jet velocity $\langle V \rangle$ of 1.38 m min⁻¹. The first take up roller speed, V , was 1.40 m min⁻¹ to give a jet stretch, $\langle V \rangle/V$, of approximately 1. The DMAc/water ratios for baths I, II, and III were 60:40, 10:90, and 0:100, respectively. Baths I and II were maintained at 30 °C, while bath III was maintained at 90 °C. No fiber drawing took place in baths I and II, while fibers were drawn 4.6 times in bath III and allowed to relax (0.94 times) in the subsequent drying process, which was carried out on a hot plate at 120 °C. The maximum achievable draw ratio for pure PAN fiber was 4.3, while fibers containing 5 and 10 wt.-% SWNTs could be drawn to a higher draw ratio. However, for a meaningful structure and properties comparison, all fibers were drawn to a draw ratio of 4.3. PAN and PAN/SWNT fibers were also prepared using DMF giving comparable results.

Fiber tensile and dynamic mechanical properties were determined using Rheometrics Scientific's solids analyzer (RSA III). The gauge length and crosshead speed for the tensile tests were 25 mm and 10 mm min⁻¹, respectively. Dynamic mechanical tests were conducted at a frequency of 10 Hz at a heating rate of 5 °C min⁻¹. Fiber shrinkage was determined using TA Instruments thermo-mechanical analyzer (TMA 2940) at 0.38 MPa pre-stress. For orientation determination, Raman spectra were collected in the back scattering geometry using a Holoprobe Research 785 Raman Microscope made by Kaiser Optical System using 785 nm excitation laser. Spectra were collected in VV configuration, where the polarizer and the analyzer are parallel to each other, and at 0, 5, 15, 30, 45, 60, 75, and 90° to the fiber axis. The SWNT orientation [19] was determined from the peak intensity of the tangential mode at $\sim 1592 \text{ cm}^{-1}$ assuming Gaussian distribution for the nanotubes, though a more rigorous method for determining SWNT orientation has now been developed [20]. The polarized infrared transmission spectra were recorded on a Perkin Elmer FTIR microscope (Autoimage system) with the polarization direction of the incident IR beam parallel and perpendicular to the fiber axis. In order to reduce the surface scattering, a single filament was pressed in KBr powder, to form a pellet for IR spectra collection. WAXD was obtained on a multifilament bundle on a Rigaku 2D SAXS/WAXS Diffraction System (Rigaku Micromax-007, 45 kV, 66 mA, $\lambda = 1.54 \text{ \AA}$) using a Rigaku R-Axis IV++ detection system. The diffraction patterns were analyzed using AreaMax V.1.00 and MDI Jade 6.1.

Received: May 28, 2003

Final version: October 3, 2003

- [1] R. H. Baughman, A. A. Zakhidov, W. A. de Heer, *Science* **2002**, 297, 787.
- [2] R. Andrews, D. Jacques, A. M. Rao, T. Rantell, F. Derbyshire, Y. Chen, J. Chen, R. C. Haddon, *Appl. Phys. Lett.* **1999**, 75, 1329.
- [3] a) M. S. P. Shaffer, A. H. Windle, *Adv. Mater.* **1999**, 11, 937. b) X.-Y. Gong, J. Liu, S. Baskaran, R. D. Voise, J. S. Young, *Chem. Mater.* **2000**, 12, 1049. c) Z.-X. Jin, K. P. Pramoda, G.-Q. Xu, S. H. Goh, *Chem. Phys. Lett.* **2001**, 337, 43.
- [4] S. Kumar, T. D. Dang, F. E. Arnold, A. R. Bhattacharyya, B. G. Min, X.-F. Zhang, R. A. Vaia, C. Park, W. W. Adams, R. H. Hauge, R. E. Smalley, S. Ramesh, P. A. Willis, *Macromolecules* **2002**, 35, 9039.
- [5] X. Zhang, T. Liu, T. V. Sreekumar, S. Kumar, V. C. Moore, R. H. Hauge, R. E. Smalley, *Nano Lett.* **2003**, 3, 1285.
- [6] J. C. Masson, *Acrylic Fiber Technology and Applications*, Marcel Dekker, New York **1995**.
- [7] W. Watt, in *Strong Fibers* (Eds: W. Watt, B. V. Perov), North-Holland, Amsterdam **1985**, Ch. 9.
- [8] T. Kowalewski, N. V. Tsarevsky, K. Matyjaszewski, *J. Am. Chem. Soc.* **2002**, 124, 10632.
- [9] C. Piriot, I. Willems, A. Fonseca, J. B. Nagy, J. Delhalle, *Adv. Eng. Mater.* **2002**, 4, 109.
- [10] a) K. D. Ausman, R. Piner, O. Lourie, R. S. Ruoff, M. Korobov, *J. Phys. Chem. B* **2000**, 104, 8911. b) J. L. Bahr, E. T. Mickelson, M. J. Bronikowski, R. E. Smalley, J. M. Tour, *Chem. Commun.* **2001**, 2, 193.
- [11] T. Liu, T. V. Sreekumar, S. Kumar, R. H. Hauge, R. E. Smalley, *Carbon* **2003**, 41, 2440.
- [12] J. Zeng, B. Saltysiak, W. S. Johnson, D. A. Schiraldi, S. Kumar, *Composites, Part B*, in press.
- [13] B. D. Cullity, *Elements of X-Ray Diffraction*, 2nd ed., Addison-Wesley Publishing Company, Reading, MA **1978**, p. 102.
- [14] R. J. Samuels, *Structured Polymer Properties: The Identification, Interpretation, and Application of Crystalline Polymer Structure*, John Wiley & Sons, New York **1974**.
- [15] M. L. Dunn, H. L. Ledbetter, P. R. Heyliger, C. S. Choi, *J. Mech. Phys. Solids* **1996**, 44, 1509.
- [16] T. Liu, S. Kumar, *Nano Lett.* **2003**, 3, 647.
- [17] T. Uchida, T. V. Sreekumar, T. Lui, S. Kumar, unpublished.
- [18] a) P. Nikolae, M. J. Bronikowski, R. K. Bradley, F. Rohmund, D. T. Colbert, K. A. Smith, R. E. Smalley, *Chem. Phys. Lett.* **1999**, 313, 91. b) I. W. Chiang, B. E. Brinson, R. E. Smalley, J. L. Margrave, R. H. Hauge, *J. Phys. Chem. B* **2001**, 105, 1157.
- [19] a) R. Haggmueller, H. H. Gommans, A. G. Rinzler, J. E. Fischer, K. I. Winey, *Chem. Phys. Lett.* **2000**, 330, 219. b) J. Hwang, H. H. Gommans, A. Ugawa, H. Tashiro, R. Haggmueller, K. I. Winey, J. E. Fischer, D. B. Tanner, A. Rinzler, *Phys. Rev. B* **2000**, 62, 13310. c) H. H. Gommans, J. W. Alldredge, H. Tashiro, J. Park, J. Magnusson, A. G. Rinzler, *J. Appl. Phys.* **2000**, 88, 2509. d) J. E. Fischer, W. Zhou, J. Vavro, M. C. Llaguno, C. Guthy, R. Haggmueller, M. J. Casavant, D. E. Walters, R. E. Smalley, *J. Appl. Phys.* **2003**, 93, 2157.
- [20] T. Liu, S. Kumar, *Chem. Phys. Lett.* **2003**, 378, 257.

Efficient Organic Blue-Light-Emitting Devices with Double Confinement on Terfluorenes with Ambipolar Carrier Transport Properties**

By Chung-Chih Wu,* Yu-Ting Lin, Ken-Tsung Wong,* Ruei-Tang Chen, and Yuh-Yih Chien

Organic light-emitting devices (OLEDs) have been the subject of intense investigation in recent years due to their applications in displays and lighting.^[1-3] In all these applications, good blue-emitting materials and devices have been essential and therefore there have been continual efforts towards exploring blue-emitting materials and devices with improved characteristics.^[4-13]

Among various blue-emitting materials reported, fluorene-based polymers or compounds have attracted wide interest in recent years as efficient blue emitters.^[14-20] In our previous studies we have found that ter(9,9-diarylfluorene)s (TDAFs) **1** and **2** (Fig. 1) exhibit some intriguing properties that are promising for blue-light-emitting devices.^[21,22] The C9-aryl

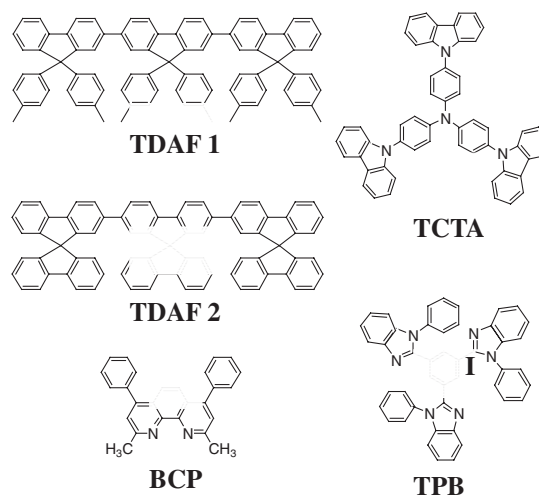


Figure 1. Chemical structures of various compounds used: TDAF **1** and **2**, TCTA, TPB, BCP.

[*] Prof. C.-C. Wu, Y.-T. Lin
Department of Electrical Engineering
Graduate Institute of Electro-optical Engineering and
Graduate Institute of Electronics Engineering
National Taiwan University
Taipei 106 (ROC)
E-mail: chungwu@cc.ee.ntu.edu.tw
Prof. K.-T. Wong, R.-T. Chen, Y.-Y. Chien
Department of Chemistry
National Taiwan University
Taipei 106 (ROC)

[**] The authors gratefully acknowledge the financial support from the National Science Council (Grant No. NSC 92-2215-E-002-011, NSC 91-2113 M-002-025) and the Ministry of Education of Republic of China.